International Journal of Solids and Structures 56–57 (2015) 126–135

Contents lists available at ScienceDirect

International Journal of Solids and Structures

journal homepage: www.elsevier.com/locate/ijsolstr

Two-dimensional chemo-elasticity under chemical equilibrium

Hamed Haftbaradaran [a], Jianmin Qu [b,*]

[a] Department of Civil Engineering, Faculty of Engineering, University of Isfahan, 81744-73441 Isfahan, Iran
[b] Department of Civil and Environmental Engineering, Department of Mechanical Engineering, Northwestern University, United States

ARTICLE INFO

Article history:
Received 11 May 2014
Received in revised form 21 October 2014
Available online 24 December 2014

Keywords:
Chemo-elasticity
Dislocation
Diffusion
Chemical potential

ABSTRACT

The coupling between solid state diffusion and mechanical stress arises in a number of important technological applications. The theory that describes such coupling is termed chemo-elasticity. In this paper, a solution approach is developed for two-dimensional chemo-elasticity problems. First, a coupled system of nonlinear partial differential equations is derived in terms of an Airy stress function and the solute concentration. Then, this coupled system of nonlinear equations is solved asymptotically using a perturbation technique. Finally, based on this approach, asymptotic solutions are obtained for three fundamental problems in two-dimensional chemo-elasticity, namely, a circular hole in an infinite plate under uniaxial tension, a straight edge dislocation and a disclination.

1. Introduction

In this paper, chemo-elasticity refers to the coupled theory of solid state diffusion and deformation in elastic solids. It deals with the thermodynamics of mechanically stressed solids that may change their composition through either solute redistribution within the solids, or mass exchange with the surrounding environment. Chemo-elasticity problems may arise in a number of technological areas including ionic solids in fuel cells (Swaminathan et al., 2007a,b), intercalation in batteries (Burch and Bazant, 2009; Bai et al., 2011; Cogswell and Bazant, 2012; Cui et al., 2012a,b, 2013a,b), and the growth of porous biogenic single crystals (Kienzler et al., 2006; Fratzl et al., 2010), just to name a few. In these applications, the solute is driven into or out of a host solid by various (electro-) chemical and mechanical deriving forces. A free-standing stress-free material element may expand (or shrink) to accommodate the solute insertion or extraction. However, such volumetric change may be restricted by either the surround materials or by the mechanical constraint imposed by the boundary conditions. Restriction to the composition-induced volumetric change will lead to mechanical stress in the solid. On the other hand, the stresses in the solid may affect solute diffusion in the solid. For instance, in thin film electrodes deposited on a substrate, the volumetric changes are restricted by the underlying current collector (Graetz et al., 2004). In the biomimetic growth of porous single crystals, cavities form and grow to accommodate significant volume reduction caused by crystallization of the amorphous precursor. However, formation of cavities gives rise to stress concentration and could increase the risk of failure (Fratzl et al., 2010). It is, therefore, of interest to investigate the interactive effects of the presence of the solute in the matrix on the mechanical stress fields.

Although chemo-elasticity problems have been investigated since the 1930s, e.g., (Fowler and Guggenheim, 1939), the development of a systematic framework is due to Larche and Cahn (1973). For a solid under chemical equilibrium, they showed that it is possible to introduce a set of modified material properties, namely open-system elastic constants, which account for the interplay between the non-uniform stress field and concentration within a linearized regime. This method hinges upon linearization of the chemical field in terms of stress components, and has been employed in the study of dislocations (Larche and Cahn, 1985; Sofronis, 1995), precipitates and inclusions (Johnson and Voorhees, 1985; King et al., 1991) and redistribution of solute in various interstitial sites in crystalline metals (Johnson and Huh, 2003; Voorhees and Johnson, 2004).

In this paper, we build upon Larche and Cahn's general framework (Larche and Cahn, 1973), and develop a solution approach to two-dimensional chemo-elasticity problems. By using the Airy stress function, we derive a coupled system of nonlinear partial differential equations for the Airy stress function and the solute concentration. Since an analytical solution does not seem to be feasible, we present a perturbation scheme that leads to an asymptotic solution for the coupled system of nonlinear equations. The small parameter $\hat{\eta}$ used in the perturbation scheme is a dimensionless parameter representing the coupling between the mechanical and chemical fields. Based on this approach, we obtain analytically the asymptotic solutions up to the second order of $\hat{\eta}$ for three

* Corresponding author.
E-mail address: j-qu@northwestern.edu (J. Qu).

http://dx.doi.org/10.1016/j.ijsolstr.2014.11.025
0020-7683/

fundamental problems in two-dimensional chemo-elasticity, namely, a circular hole in an infinite plate under uniaxial tension, a straight edge dislocation and a disclination. We also demonstrate that, for traction-prescribed problems, the leading order term in our asymptotic solution is equivalent to the solution obtained by Larche and Cahn (1973) using the open-system elastic constant approach.

The paper is arranged as follows. In Section 2, we derive the three-dimensional governing equations in chemo-elasticity. The corresponding two-dimensional equations are derived in Section 3 by introducing an Airy stress function. This system of two-dimensional equations are solved in Section 4 by an asymptotic approach whereby the field quantities are expanded in terms of the perturbation parameter $\hat{\eta}$. This asymptotic approach allows us to reduce the governing coupled nonlinear equations into a set of linear decoupled equations which can be solved recursively to obtain the higher order elastic and concentration fields. Using this asymptotic perturbation method, we investigate the disturbance of the concentration field as well as the elastic fields caused by the emergence of a hole, dislocation, and disclination under plane stress and/or plane strain conditions in an infinite medium. The connection between the asymptotic approach and the method of open-system material constants is also discussed. Finally, in Section 5, we conclude by summarizing the main findings of this work.

2. Governing equations for solid state diffusion

Without loss of generality, we consider an elastic solid A_xB that consists of species A and species B. It is assumed that the concentration of A in A_xB may vary from $x = 0$ to $x = x_{\max}$, where $x_{\max}$ is the solvability of A in B. One may also view species A as the solute and species B as the solvent. Furthermore, we assume that the solid in consideration can be represented by the network model of Larche and Cahn (1973), namely, the lattice sites of species B form a network within which species A can move (diffuse). This allows the definition of a displacement field and hence a strain field of the solid. To simplify the mathematics, we will only consider small strain deformation in the rest of this paper.

In the following, it is convenient to define molar concentration of the solute per unit volume of the solvent as $c = x/V_m$, where V_m is the molar volume of the pure solvent in its stress-free state. We assume that the solute-free solvent corresponds to a stress-free state, and the compositional change of the mixture causes a volumetric deformation according to

$$\varepsilon^c_{ij} = \eta x \delta_{ij} = \eta V_m c \delta_{ij}, \tag{1}$$

where δ_{ij} is the Kronecker delta, η is the coefficient of compositional expansion (CCE), which is a material property that characterizes the linear measure of the volumetric change due to unit change of the composition (Swaminathan et al., 2007a,b). For a given material, the CCE can be obtained either experimentally, or by conducting molecular dynamic simulations (Swaminathan and Qu, 2009; Cui et al., 2012a,b,c). The total strain caused by the compositional change and applied load can be written as

$$\varepsilon_{ij} = \frac{1}{2}(u_{i,j} + u_{j,i}) = \varepsilon^e_{ij} + \varepsilon^c_{ij}, \tag{2}$$

where u_i is the displacement and ε^e_{ij} is the elastic strain. The total strain needs to satisfy the compatibility condition,

$$\varepsilon_{pki}\varepsilon_{qlj}\varepsilon_{ij,kl} = 0, \tag{3}$$

where ε_{pki} is the permutation symbol.

We further assume that the solid is linear elastic so that its elastic state is uniquely determined by the elastic strain energy function

$$w = \frac{E}{2(1+\nu)}\left(\varepsilon^e_{ij}\varepsilon^e_{ij} + \frac{\nu \varepsilon^e_{kk}\varepsilon^e_{mm}}{1-2\nu}\right), \tag{4}$$

and the stress tensor is thus given by

$$\sigma_{ij} = \frac{\partial w}{\partial \varepsilon^e_{ij}} = \frac{E}{(1+\nu)}\left(\varepsilon^e_{ij} + \frac{\nu \varepsilon^e_{kk}}{1-2\nu}\delta_{ij}\right), \tag{5}$$

where E and ν are the Young's modulus and Poisson's ratio, respectively, of the solid, which are assumed to be independent of the solute concentration. This assumption is valid for most solids under dilute solute concentration. Eq. (5) can be inverted to give

$$\varepsilon^e_{ij} = \frac{1}{E}[(1+\nu)\sigma_{ij} - \nu\sigma_{kk}\delta_{ij}]. \tag{6}$$

In the absence of body forces, the stress needs to satisfy the static equilibrium equations,

$$\frac{\partial \sigma_{ji}}{\partial x_j} = 0. \tag{7}$$

In this stressed-solid, the chemical potential of species A will depend on the stress (Larche and Cahn, 1973). By assuming small strain and composition-independent isotropic elasticity, the stress-dependent chemical potential (more precisely, the diffusion potential of species A in species B) can be derived from the general expression of (Swaminathan et al., 2007a,b; Cui et al., 2012a,b,c),

$$\mu = \mu_0 + R_g T \log\frac{c}{c_{\max} - c} - V_m \eta \sigma_{kk}, \tag{8}$$

where μ_0 is a constant representing the chemical potential at a standard state, R_g is the standard gas constant, T is the absolute temperature, c is the molar concentration of the solute, and $c_{\max} = x_{\max}/V_m$ corresponds to the saturation state of the solution. The particular choice of the potential ensures that the stoichiometric state has the lowest energy (i.e., $\mu \to -\infty$ as $c \to 0$), and the state of saturation has the highest energy (i.e., $\mu \to \infty$ as $c \to c_{\max}$).

The governing equations presented above are valid within the elastic solid of interest. The stress and solute concentration within the solid depend also on what happens at the boundary of the solid. Therefore, boundary conditions are required in order to uniquely determine the stress and solute concentration fields.

Consider an elastic solid Ω with surface S with outward unit normal vector n_i. As usual, the mechanical boundary conditions can be prescribed as

$$\sigma_{ij}n_i\big|_{S_\sigma} = p_j, \quad u_i\big|_{S_u} = U_i, \tag{9}$$

where $S_u + S_\sigma = S$ and p_j and U_i are, respectively, the prescribed traction and displacement on the boundary. The chemical boundary conditions can be specified as

$$\mu\big|_{S_\mu} = \mu_s, \quad -\frac{cD}{R_g T}\nabla\tilde{\mu}\Big|_{S_J} = \mathbf{J}_s, \tag{10}$$

where $S_\mu + S_J = S$, and μ_s and $\mathbf{J}_s$ are, respectively, the prescribed chemical potential and the flux on the boundary.

3. Two-dimensional plane problems under electrochemical equilibrium

We assume that all field quantities are functions of x_1 and x_2 only, i.e.,

$$u_1 = u_1(x_1, x_2), \quad u_2 = u_2(x_1, x_2), \quad u_3 = u_3(x_1, x_2), \quad c = c(x_1, x_2). \tag{11}$$

Further, for plane strain, we assume

$$\varepsilon_{33} = \varepsilon_{23} = \varepsilon_{13} = 0. \tag{12}$$

And, for plane stress, we assume

$$\sigma_{33} = \sigma_{23} = \sigma_{13} = 0. \tag{13}$$

In both cases, the Hooke's law given in (6) in conjunction with (1) is reduced to

$$\begin{bmatrix} \varepsilon_{11} \\ \varepsilon_{22} \end{bmatrix} = \frac{1 - sv^2}{E} \begin{bmatrix} 1 & -v/(1-sv) \\ -v/(1-sv) & 1 \end{bmatrix} \begin{bmatrix} \sigma_{11} \\ \sigma_{22} \end{bmatrix} + (1+sv)\eta V_m c \begin{bmatrix} 1 \\ 1 \end{bmatrix}, \tag{14}$$

$$\varepsilon_{12} = \frac{\sigma_{12}(1+v)}{E}, \quad \sigma_{33} = s[v(\sigma_{11}+\sigma_{22}) - E\eta V_m c], \tag{15}$$

where, the parameter $s = 0$ for plane stress, and $s = 1$ for plane strain.

Furthermore, the total strain needs to satisfy the compatibility equation (3), which is reduced to only one non-trivial equation,

$$\frac{\partial^2 \varepsilon_{11}}{\partial x_2^2} - 2\frac{\partial^2 \varepsilon_{12}}{\partial x_1 \partial x_2} + \frac{\partial^2 \varepsilon_{22}}{\partial x_1^2} = 0. \tag{16}$$

Let us now introduce the Airy stress function $\varphi(x_1, x_2)$ by

$$\sigma_{11} = \frac{\partial^2 \varphi}{\partial x_2^2}, \quad \sigma_{22} = \frac{\partial^2 \varphi}{\partial x_1^2}, \quad \sigma_{12} = -\frac{\partial^2 \varphi}{\partial x_1 \partial x_2}. \tag{17}$$

With the help of (14)–(17) and (2), we can rewrite (16) as

$$\nabla^4 \varphi + \eta V_m \frac{E}{1-sv} \nabla^2 c = 0. \tag{18}$$

Next, consider the case when the chemical field is in equilibrium, i.e., the chemical potential given by (8) is a constant μ_{eq} over the entire domain and independent of time, i.e.,

$$\mu_{eq} - \mu_0 = R_g T \log \frac{c}{c_{\max} - c} - V_m \eta \sigma_{kk} = \text{constant}, \tag{19}$$

where, according to (17) and the second of (15), the hydrostatic stress in (19) can be expressed as

$$\sigma_{kk} = (1+sv)\nabla^2 \varphi - sE\eta V_m c. \tag{20}$$

We now have derived a system of two partial differential equations, (18) and (19), for the two unknowns, φ and c. In conjunction with the boundary conditions (9) and (10), they form a boundary value problem for the field quantities φ and c. Once φ and c are known for a given set of boundary conditions, the corresponding two-dimensional chemo-elasticity problem under chemical equilibrium can be obtained, because the corresponding stress, strain and displacement fields can be obtained from φ and c by using (17), (14) and (2).

We note that the boundary value problem for φ and c is nonlinear due to the nonlinear relationship between the solute concentration c and the hydrostatic stress σ_{kk}. Proving the existence and uniqueness of this nonlinear boundary value problem rigorously is beyond the scope of the present study. Nevertheless, engineering intuition seems to indicate that the solution to certain boundary conditions should exist and unique. In what follows, we will investigate such solutions for a few important engineering problems.

To this end, we rewrite the governing equations (19) and (18) into the following dimensionless form,

$$\hat{\eta}(1+sv)\bar{\nabla}^2 \hat{\varphi} - s\hat{\eta}\bar{c}_{\max}\hat{c} = \log\frac{\hat{c}}{1-\hat{c}} - \log\frac{\hat{c}_{eq}}{1-\hat{c}_{eq}}, \tag{21}$$

$$(1-sv)\bar{\nabla}^4 \hat{\varphi} + \bar{c}_{\max}\bar{\nabla}^2 \hat{c} = 0, \tag{22}$$

where

$$\hat{c} = \frac{c}{c_{\max}}, \quad \hat{\varphi} = \frac{\varphi}{E\ell^2}, \quad \hat{\eta} = \frac{\eta V_m E}{RT}, \quad \bar{c}_{\max} = \eta V_m c_{\max},$$
$$\bar{\mu}_{eq} = \frac{\mu_{eq} - \mu_0}{R_g T}, \quad \hat{c}_{eq} = \frac{e^{\bar{\mu}_{eq}}}{1 + e^{\bar{\mu}_{eq}}}, \tag{23}$$

where $\hat{c}_{eq}$ is essentially the solute concentration in the absence of the stress, and ℓ is a characteristic length pertinent to the problem. The barred harmonic and biharmonic operators operate with respect to the spatial coordinates normalized by the length scale ℓ. By solving this system of equations, one can obtain the dimensionless solute concentration $\hat{c}$, and the dimensionless Airy stress function $\hat{\varphi}$.

Once the dimensionless stress function $\hat{\varphi}$ and solute concentration $\hat{c}$ are known, the corresponding strain field can be obtained from (14) and (15). Integrating (14) gives the expressions of the displacements u_1 and u_2. As a result of the integrations, the expressions of u_1 and u_2 contain unknown functions $f(x_2)$ and $g(x_1)$, respectively. Substituting u_1 and u_2 into (15) yields two second order ordinary differential equations for $f(x_2)$ and $g(x_1)$, respectively. Solutions of these differential equations with proper boundary conditions provide the complete solution to the chemo-elasticity problem. Detailed steps in obtaining the displacement fields in polar coordinate systems are discussed in Appendix B.

Under chemical equilibrium, the flux vanishes. Thus, the only nontrivial chemical boundary condition is the first of (10), which can be written as

$$\left(\mu_0 + R_g T \log\frac{c}{c_{\max} - c} - V_m \eta \sigma_{kk}\right)\Big|_S = \mu_{eq}. \tag{24}$$

The mechanical boundary conditions (9) still hold. Clearly, this system is highly nonlinear. Explicit analytical solution does not seem to be possible. In Section 4, we will attempt an asymptotic solution for small $\hat{\eta}$.

Before closing this section, we remark that the chemical equilibrium condition (19) means that the system under consideration is open to and maintains in equilibrium with a reservoir of infinite extent that maintains a constant chemical potential μ_{eq}. Therefore, μ_{eq} represents the magnitude of the chemical loading. Further, condition (19) means

$$c = c_{\max} \exp\left(\frac{\mu_{eq} - \mu_0 + \eta V_m \sigma_{kk}}{R_g T}\right)\left[1 + \exp\left(\frac{\mu_{eq} - \mu_0 + \eta V_m \sigma_{kk}}{R_g T}\right)\right]^{-1}. \tag{25}$$

In other words, the concentration is bounded by $0 < c < c_{\max}$, unless the hydrostatic stress has singularities ($\to \pm\infty$), in which case, $c = 0$ and/or $c = c_{\max}$ may be possible.

4. Asymptotic solutions of two-dimensional plane problems under chemical equilibrium

We begin with the ansatz,

$$\hat{c} = \hat{c}_{eq}(1 + \hat{c}_1\hat{\eta} + \hat{c}_2\hat{\eta}^2 + \cdots), \quad \hat{\varphi} = \hat{\varphi}_0 + \hat{\varphi}_1\hat{\eta} + \hat{\varphi}_2\hat{\eta}^2 + \cdots. \tag{26}$$

Next, substituting (26) into (21) and (22), and expanding the logarithm function into power series of $\hat{\eta}$. Then, in the resulting equations setting $\hat{\eta} = 0$ yields,

$$\bar{\nabla}^4 \hat{\varphi}_0 = 0, \tag{27}$$

setting the coefficient of $\hat{\eta}$ to zero yields

$$(1+sv)\bar{\nabla}^2 \hat{\varphi}_0 - s\bar{c}_{\max}\hat{c}_{eq} = \frac{\hat{c}_1}{1-\hat{c}_{eq}}, \tag{28}$$

$$(1-sv)\bar{\nabla}^4 \hat{\varphi}_1 + \bar{c}_{\max}\hat{c}_{eq}\bar{\nabla}^2 \hat{c}_1 = 0, \tag{29}$$

and setting the coefficient of $\hat{\eta}^2$ to zero yields

$$(1+sv)\bar{\nabla}^2\hat{\varphi}_1 - s\bar{c}_{\max}\hat{c}_{eq}\hat{c}_1 = \frac{\hat{c}_2}{1-\hat{c}_{eq}} - \frac{1-2\hat{c}_{eq}}{2(1-\hat{c}_{eq})^2}\hat{c}_1^2, \tag{30}$$

$$(1-sv)\bar{\nabla}^4\hat{\varphi}_2 + \bar{c}_{\max}\hat{c}_{eq}\bar{\nabla}^2\hat{c}_2 = 0. \tag{31}$$

Equations for higher order terms can be similarly derived.

It can be easily shown that (27)–(31) reduce to

$$\bar{\nabla}^4\hat{\varphi}_0 = 0, \quad \hat{c}_1 = (1-\hat{c}_{eq})\left[(1+sv)\bar{\nabla}^2\hat{\varphi}_0 - s\bar{c}_{\max}\hat{c}_{eq}\right], \tag{32}$$

$$\bar{\nabla}^4\hat{\varphi}_1 = 0, \quad \hat{c}_2 = (1-\hat{c}_{eq})[(1+sv)\bar{\nabla}^2\hat{\varphi}_1 - s\bar{c}_{\max}\hat{c}_{eq}\hat{c}_1] + \frac{1-2\hat{c}_{eq}}{2(1-\hat{c}_{eq})}\hat{c}_1^2, \tag{33}$$

$$\bar{\nabla}^4\hat{\varphi}_2 = -\frac{\bar{c}_{\max}\hat{c}_{eq}(1-2\hat{c}_{eq})}{2(1-sv)(1-\hat{c}_{eq})}\bar{\nabla}^2\hat{c}_1^2. \tag{34}$$

Clearly, these equations are linear. More importantly, the mechanical and chemical fields are decoupled for $\hat{\varphi}_0$ and $\hat{\varphi}_1$ in that their governing equations are independent of the solute concentration. In fact, their governing equations are identical to the two-dimensional elasticity equations. Therefore, one can take advantage of the known elasticity solutions. Once $\hat{\varphi}_0$ and $\hat{\varphi}_1$ are known, the solute concentration $\hat{c}_1$ and $\hat{c}_2$ can be evaluated without the need of solving any additional equations. In other words, once the elasticity solutions are known, the corresponding chemo-elasticity solutions can be obtained without solving additional equations. Of course, to obtain the second order stress fields, Eq. (34) will need to be solved.

We also note that the governing equations for the stress functions $\hat{\varphi}_0$ and $\hat{\varphi}_1$ are identical to their counterparts in two-dimensional elasticity. It then follows from (17) that the corresponding stresses should also be the same as their counterparts in two-dimensional elasticity. This seems to indicate that the two leading order terms in the stress field are decoupled from the solute concentration c. However, this is true only for problems under prescribed traction boundary conditions, where the equilibrium equations can be solved without invoking the constitutive equations. For problems under displacement-boundary conditions, the equilibrium equations will need to be solved in conjunction with the constitutive equations (14) and (15), which results in the coupling between the stresses and the solute concentration c.

In the following, we will follow the approach outlined above to derive the solutions to some chemo-elasticity problems that have well-known corresponding elasticity solutions.

4.1. A Circular hole in a tensile field under chemical equilibrium

Consider a plate of infinite extent containing a circular hole of radius a. Let the plate be subjected to a uniform tension σ^∞ in the x_2-direction, see Fig. 1. Further, we assume that the plate is embedded in an infinite reservoir so that it maintains a uniform chemical potential $\bar{\mu}_{eq}$ throughout. It then follows from (19) that

$$\bar{\mu}_{eq} = \log\frac{\hat{c}^\infty}{1-\hat{c}^\infty} - \hat{\eta}\frac{\sigma^\infty}{E} = \log\frac{\hat{c}_{eq}}{1-\hat{c}_{eq}}, \tag{35}$$

where $c^\infty = \hat{c}^\infty c_{\max}$ is the solute concentration far away from the hole, and $\hat{c}_{eq}$ is the concentration in the absence of the stress. Our goal is to find the non-uniform distributions of stress and solute concentration near the hole under chemical and mechanical equilibrium. Since it is a plate, we will consider the deformation to be plane stress, i.e., $s = 0$.

For convenience, we have introduced the dimensionless polar coordinates ρ and θ such that $x_1 = \ell\rho\cos\theta$ and $x_2 = \ell\rho\sin\theta$, and

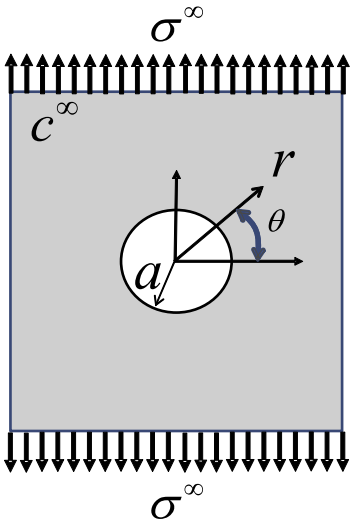

Fig. 1. A plate with a circular hole subject to uniaxial tension.

the radius of the hole is taken as the characteristic length in (23), i.e. $\ell = a$. Therefore, the boundary conditions are

$$\sigma_{rr}|_{\rho\to\infty} = \frac{\sigma^\infty}{2}(1-\cos 2\theta), \quad \sigma_{\theta\theta}|_{\rho\to\infty} = \frac{\sigma^\infty}{2}(1+\cos 2\theta),$$
$$\sigma_{r\theta}|_{\rho\to\infty} = \frac{\sigma^\infty}{2}\cos 2\theta, \tag{36}$$

$$\sigma_{rr}|_{\rho\to 1} = 0, \quad \sigma_{r\theta}|_{\rho\to 1} = 0, \quad \hat{c}|_{\rho\to\infty} = \hat{c}^\infty. \tag{37}$$

Taking advantage of the known elasticity solution for a hole under tension, we anticipate that

$$\hat{\varphi}_0 = \frac{\hat{\sigma}^\infty\rho^2}{4}(1+\cos 2\theta) - \frac{\hat{\sigma}^\infty}{2}\log\rho - \frac{\hat{\sigma}^\infty}{2}\left(1-\frac{1}{2\rho^2}\right)\cos 2\theta, \tag{38}$$

where $\hat{\sigma}^\infty = \frac{\sigma^\infty}{E}$. It can be shown by substitution that $\hat{\varphi}_0$ is a biharmonic function that satisfies the first of (32). The corresponding stress components are

$$\sigma_{rr}^{(0)} = \frac{\sigma^\infty}{2}\left(1-\frac{1}{\rho^2}\right) - \frac{\sigma^\infty}{2}\left(1-\frac{4}{\rho^2}+\frac{3}{\rho^4}\right)\cos 2\theta, \tag{39}$$

$$\sigma_{\theta\theta}^{(0)} = \frac{\sigma^\infty}{2}\left(1+\frac{1}{\rho^2}\right) + \frac{\sigma^\infty}{2}\left(1+\frac{3}{\rho^4}\right)\cos 2\theta, \tag{40}$$

$$\sigma_{r\theta}^{(0)} = \frac{\sigma^\infty}{2}\left(1+\frac{2}{\rho^2}-\frac{3}{\rho^4}\right)sin2\theta. \tag{41}$$

Consequently, the second of (32) yields

$$\hat{c}_1 = (1-\hat{c}_{eq})\left(1+\frac{2\cos 2\theta}{\rho^2}\right)\frac{\sigma^\infty}{E}. \tag{42}$$

It can be easily verified that the above stress fields satisfy the boundary conditions at infinity $\rho\to\infty$, and at the traction-free surface of the hole $\rho = 1$ as stated in (36) and (37). The stresses corresponding to $\hat{\varphi}_1$ must then satisfy homogeneous boundary conditions at both $\rho\to\infty$ and $\rho = 1$. Since $\hat{\varphi}_1$ must also satisfy the homogeneous biharmonic equation, see the first of (33), one can conclude that

$$\hat{\varphi}_1 = 0, \sigma_{rr}^{(1)} = \sigma_{\theta\theta}^{(1)} = \sigma_{r\theta}^{(1)} = 0. \tag{43}$$

This result indicates that the presence of the chemical field does not affect the stress field up to the first order in $\hat{\eta}$. It is shown in

Appendix A that the leading order solutions (39)–(42) are consistent with the results of Larche and Cahn (1985).

The second of (33) suggests that

$$\hat{c}_2 = \frac{1}{2}(1-\hat{c}_{eq})(1-2\hat{c}_{eq})\left(1+\frac{2\cos 2\theta}{\rho^2}\right)^2\left(\frac{\sigma^\infty}{E}\right)^2. \tag{44}$$

To obtain the second order stress field around the hole, one needs to solve (34). By making use of (44), we can recast (34) into

$$\bar{\nabla}^4\hat{\varphi}_2 = -16\bar{c}_{\max}\hat{c}_{eq}(1-\hat{c}_{eq})(1-2\hat{c}_{eq})\left(\frac{\sigma^\infty}{E}\right)^2\frac{1}{\rho^6}. \tag{45}$$

The solution of (45), satisfying the zero traction boundary conditions at $\rho = 1$ and $\rho \to \infty$, is

$$\hat{\varphi}_2 = -\bar{c}_{\max}\hat{c}_{eq}(1-\hat{c}_{eq})(1-2\hat{c}_{eq})\left(\frac{\sigma^\infty}{E}\right)^2\left(\frac{1}{4\rho^2}+\frac{1}{2}\log\rho\right), \tag{46}$$

which leads to the following stress fields,

$$\sigma^{(2)}_{rr} = -\bar{c}_{\max}\hat{c}_{eq}(1-\hat{c}_{eq})(1-2\hat{c}_{eq})\frac{\sigma^{\infty 2}}{E}\frac{1}{2\rho^2}\left(1-\frac{1}{\rho^2}\right), \tag{47}$$

$$\sigma^{(2)}_{\theta\theta} = -\bar{c}_{\max}\hat{c}_{eq}(1-\hat{c}_{eq})(1-2\hat{c}_{eq})\frac{\sigma^{\infty 2}}{E}\frac{1}{2\rho^2}\left(\frac{3}{\rho^2}-1\right), \tag{48}$$

$$\sigma^{(2)}_{r\theta} = 0. \tag{49}$$

Now let us focus on the hoop stress $\sigma_{\theta\theta}$, and the solute concentration c,

$$\sigma_{\theta\theta} = \sigma^{(0)}_{\theta\theta} + \sigma^{(2)}_{\theta\theta}\hat{\eta}^2, \quad \hat{c} = \hat{c}_{eq}(1+\hat{c}_1\hat{\eta}+\hat{c}_2\hat{\eta}^2), \tag{50}$$

where

$$\hat{c}_{eq} = \frac{e^{\bar{\mu}_{eq}}}{1+e^{\bar{\mu}_{eq}}} = \frac{\hat{c}^\infty}{e^{\frac{\hat{\eta}\sigma^\infty}{E}} + \left(1-e^{\frac{\hat{\eta}\sigma^\infty}{E}}\right)\hat{c}^\infty}. \tag{51}$$

The expressions given in (50) can be further simplified by expanding $\hat{c}_{eq}$ given in (51) into power series of $\hat{\eta}$, and retaining only terms up to the order of $\hat{\eta}^2$. Thus,

$$\frac{\sigma_{\theta\theta}}{\sigma^\infty} = \frac{1}{2}\left(1+\frac{1}{\rho^2}\right)+\frac{1}{2}\left(1+\frac{3}{\rho^4}\right)\cos 2\theta - \bar{c}_{\max}\hat{c}^\infty(1-\hat{c}^\infty)(1-2\hat{c}^\infty)\frac{\sigma^\infty}{E}\frac{1}{2\rho^2}\left(\frac{3}{\rho^2}-1\right)\hat{\eta}^2, \tag{52}$$

$$\frac{\hat{c}}{\hat{c}^\infty} = 1+2(1-\hat{c}^\infty)\frac{\hat{\eta}\sigma^\infty}{E}\frac{\cos 2\theta}{\rho^2} + 2(1-\hat{c}^\infty)(1-2\hat{c}^\infty)\left(\frac{\hat{\eta}\sigma^\infty}{E}\frac{\cos 2\theta}{\rho^2}\right)^2. \tag{53}$$

Several observations can be made. First, note that the stress concentration factor, i.e. the ratio of the maximum hoop stress which occurs at $\rho = 1$, $\theta = 0$ over the far field stress σ^∞,

$$\left.\frac{\sigma_{\theta\theta}}{\sigma^\infty}\right|_{\rho=1,\ \theta=0} = 3-\bar{c}_{\max}\hat{c}^\infty(1-\hat{c}^\infty)(1-2\hat{c}^\infty)\frac{\sigma^\infty}{E}\hat{\eta}^2, \tag{54}$$

is smaller than 3 only when $\hat{c}^\infty < 0.5$, suggesting that the chemical field could both magnify or attenuate the stress concentration depending on the magnitude of the far-field solute concentration. Second, appearance of the hole disturbs the solute distribution, and creates a "concentration" of the solute concentration near the hole. To the leading order, the concentration factor of the solute concentration near the hole is $2(1-\hat{c}^\infty)\hat{\eta}\sigma^\infty/E$, which occurs at $\theta = 0$ and $\theta = \pi$. The disturbance of the hole decays as $1/\rho^2$, and the solute concentration, as expected, approaches the prescribed value $\hat{c}^\infty c_{\max}$ as $\rho \to \infty$. Third, the second order effect of the stress on concentration is always positive if the prescribed initial solute concentration is less than half of the solvability, i.e. $\hat{c}^\infty < 0.5$, or vice versa. Fourth, if the prescribed initial solute concentration is $c_{\max}$, i.e., $\hat{c}^\infty \to 1$, then the concentration will remain as $c_{\max}$ without being disturbed by the hole, unless the applied stress field is infinite. Clearly, this theoretical limit is not possible under the chemical condition unless the applied stress is infinite, see (25). Finally, it is clear that the appearance of a hole will not disturb the solute concentration unless a stress is applied.

To visualize the effect of the hole, the variation of solute concentration on the hole surface $\hat{c}(a,\theta)/\hat{c}^\infty$ is plotted as a function of θ in Fig. 2. The solid line is for the case when the mechanical and chemical fields are decoupled, i.e., $\hat{\eta} = 0$. The dashed lines are for $\hat{\eta}\sigma^\infty/E = 0.1$, and $\hat{c}^\infty = 0.1$ and $\hat{c}^\infty = 0.6$, respectively. It is seen that the concentration at $\theta = 0$ is amplified by the tensile stress, while the concentration at $\theta = \pi/2$ is attenuated by the compressive hydrostatic stress.

4.2. An edge dislocation under chemical equilibrium

Consider a large elastic solid containing a straight edge dislocation of Burgers vector b in the x_2-direction. Let the dislocation core be located at $x_1 = x_2 = 0$, and the line of dislocation is perpendicular to the x_1–x_2 plane. Further, we assume that the solid is embedded in an infinite reservoir so that the solute concentration far away from the dislocation core is given by $c^\infty = \hat{c}^\infty c_{\max}$. Here we consider plane strain conditions, i.e., $s = 1$. Thus, the far-field in-plane stresses vanish, and the only non-zero component of stress is $\sigma_{33} = -E\bar{c}_{\max}\hat{c}^\infty$. It follows from (19) that

$$\bar{\mu}_{eq} = \log\frac{\hat{c}^\infty}{1-\hat{c}^\infty} + \hat{\eta}\bar{c}_{\max}\hat{c}^\infty = \log\frac{\hat{c}_{eq}}{1-\hat{c}_{eq}}. \tag{55}$$

This equation establishes the relation between the far field concentration $\hat{c}^\infty$, and the stress-free equilibrium concentration $\hat{c}_{eq}$. Our goal is to find the non-uniform distributions of stress and solute concentration near the dislocation under chemical and mechanical equilibrium.

Since the Burgers vector is in the x_2-direction, the displacement field needs to satisfy the following displacement jump condition

$$u_\theta(r,0) - u_\theta(r,2\pi) = b. \tag{56}$$

Motivated by the known elasticity solution, we consider

$$\hat{\varphi}_0 = -\frac{1}{4\pi(1-\nu^2)}\rho\cos\theta\log\rho, \tag{57}$$

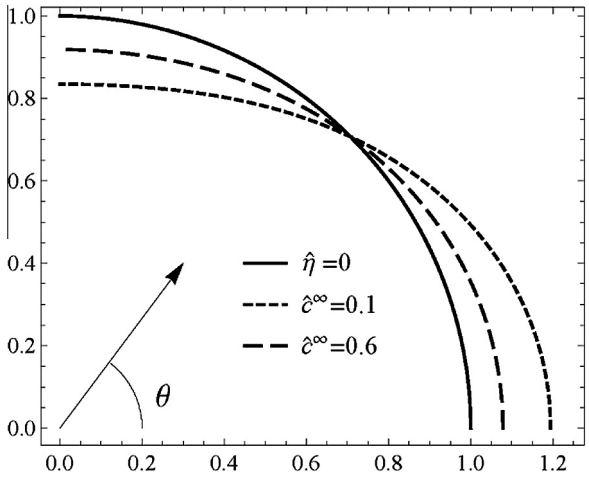

Fig. 2. Solute concentration on the hole surface.

which satisfies the first of (32). Naturally, we choose b, the magnitude of the Burgers vector, as the characteristic length, i.e. $\ell = b$. Hence $x_1 = b\rho\cos\theta$, $x_2 = b\rho\sin\theta$. The corresponding stresses are

$$\sigma_{rr}^{(0)} = \sigma_{\theta\theta}^{(0)} = -\frac{E}{4\pi\rho(1-\nu^2)}\cos\theta,$$
$$\sigma_{r\theta}^{(0)} = -\frac{E}{4\pi(1-\nu^2)\rho}\sin\theta. \tag{58}$$

It follows from Appendix B that the corresponding displacements are

$$u_r^{(0)} = \frac{b\cos\theta}{8\pi(1-\nu)} - \frac{b\theta\sin\theta}{2\pi} - \frac{b(1-2\nu)\cos\theta\log\rho}{4\pi(1-\nu)} + b(1+\nu)\bar{c}_{\max}\hat{c}_{eq}\rho, \tag{59}$$

$$u_\theta^{(0)} = \frac{b}{8\pi(1-\nu)}\sin\theta - \frac{b}{2\pi}\theta\cos\theta + \frac{b(1-2\nu)}{4\pi(1-\nu)}\sin\theta\log\rho. \tag{60}$$

We note that the last term in (59) represents a uniform deformation induced by the uniform solute concentration c_{eq}.

The first order concentration field follows directly from substituting (57) into the second of (32),

$$\hat{c}_1 = -(1-\hat{c}_{eq})\left[\frac{1}{2\pi(1-\nu)}\frac{\cos\theta}{\rho} + \bar{c}_{\max}\hat{c}_{eq}\right]. \tag{61}$$

To obtain the first order stress field, we notice that according to the first of (33), $\hat{\varphi}_1$ must be biharmonic. By trial and error, we found that

$$\hat{\varphi}_1 = -\frac{1+\nu}{1-\nu}\bar{c}_{\max}\hat{c}_{eq}(1-\hat{c}_{eq})\hat{\varphi}_0, \tag{62}$$

which is obviously biharmonic. Thus, the first order stresses are simply

$$\left[\sigma_{rr}^{(1)}, \sigma_{r\theta}^{(1)}, \sigma_{\theta\theta}^{(1)}\right] = -\frac{1+\nu}{1-\nu}\bar{c}_{\max}\hat{c}_{eq}(1-\hat{c}_{eq})\left[\sigma_{rr}^{(0)}, \sigma_{r\theta}^{(0)}, \sigma_{\theta\theta}^{(0)}\right]. \tag{63}$$

The corresponding displacements can be calculated following the approach outlined in Appendix B,

$$u_r^{(1)} = -\frac{b(1+\nu)}{8\pi(1-\nu)^2}\bar{c}_{\max}\hat{c}_{eq}(1-\hat{c}_{eq})(1+2\log\rho)\cos\theta - b(1+\nu)(\bar{c}_{\max}\hat{c}_{eq})^2(1-\hat{c}_{eq})\rho, \tag{64}$$

$$u_\theta^{(1)} = -\frac{b(1+\nu)}{8\pi(1-\nu)^2}\bar{c}_{\max}\hat{c}_{eq}(1-\hat{c}_{eq})(1-2\log\rho)\sin\theta. \tag{65}$$

Here it is noteworthy to point out that the displacement field is single-valued. Except for a uniform strain field, the first order solution obtained above can also be obtained by the method of open-system elastic constants of Larche and Cahn (1973), see Appendix A.

To obtain the second order solution, we substitute (61) and (62) into the second of (33),

$$\hat{c}_2 = \frac{(1-\hat{c}_{eq})\hat{c}_{eq}\bar{c}_{\max}}{2\pi(1-\nu)^2}(3-\nu-2\hat{c}_{eq}(2-\nu))\frac{\cos\theta}{\rho} + \frac{1}{2}(1-\hat{c}_{eq})(3-4\hat{c}_{eq})(\bar{c}_{\max}\hat{c}_{eq})^2 + \frac{(1-\hat{c}_{eq})(1-2\hat{c}_{eq})}{8\pi^2(1-\nu)^2}\left(\frac{\cos\theta}{\rho}\right)^2. \tag{66}$$

The second order stress function must satisfy (34),

$$\bar{\nabla}^4\hat{\varphi}_2 = -\bar{c}_{\max}\hat{c}_{eq}\frac{(1-\hat{c}_{eq})(1-2\hat{c}_{eq})}{4\pi^2(1-\nu)^3}\frac{1}{\rho^4}. \tag{67}$$

A particular solution to the above inhomogeneous biharmonic equation is given by

$$\hat{\varphi}_2^p = -\bar{c}_{\max}\hat{c}_{eq}\frac{(1-\hat{c}_{eq})(1-2\hat{c}_{eq})}{32\pi^2(1-\nu)^3}(\log\rho)^2. \tag{68}$$

Again, through trial and error, we found that

$$\hat{\varphi}_2 = \frac{\bar{c}_{\max}^2\hat{c}_{eq}^2(1+\nu)}{(1-\nu)^2}(1-\hat{c}_{eq})[3-\nu-2\hat{c}_{eq}(2-\nu)]\hat{\varphi}_0 + \hat{\varphi}_2^p, \tag{69}$$

renders a second order displacement field which is continuous across the slip plane. The associated second order stress and displacement fields are

$$\sigma_{rr}^{(2)} = \frac{\bar{c}_{\max}\hat{c}_{eq}(1-\hat{c}_{eq})}{(1-\nu)^3}\left[\bar{c}_{\max}\hat{c}_{eq}(1-\nu^2)[3-\nu-2\hat{c}_{eq}(2-\nu)]\sigma_{rr}^{(0)} - \frac{(1-2\hat{c}_{eq})E}{16\pi^2\rho^2}\log\rho\right], \tag{70}$$

$$\sigma_{\theta\theta}^{(2)} = \frac{\bar{c}_{\max}\hat{c}_{eq}(1-\hat{c}_{eq})}{(1-\nu)^3}\left[\bar{c}_{\max}\hat{c}_{eq}(1-\nu^2)[3-\nu-2\hat{c}_{eq}(2-\nu)]\sigma_{\theta\theta}^{(0)} - \frac{(1-2\hat{c}_{eq})E}{16\pi^2\rho^2}(1-\log\rho)\right], \tag{71}$$

$$\sigma_{r\theta}^{(2)} = \frac{(\bar{c}_{\max}\hat{c}_{eq})^2(1-\hat{c}_{eq})}{(1-\nu)^2}(1+\nu)[3-\nu-2\hat{c}_{eq}(2-\nu)]\sigma_{r\theta}^{(0)}, \tag{72}$$

and the corresponding displacements are

$$u_r^{(2)} = \frac{b\bar{c}_{\max}\hat{c}_{eq}(1+\nu)(1-\hat{c}_{eq})}{16\pi^2(1-\nu)^3\rho}(1-2\hat{c}_{eq})[\log\rho-(1-\nu)\cos(2\theta)] + \frac{b(\bar{c}_{\max}\hat{c}_{eq})^2(1+\nu)(1-\hat{c}_{eq})}{8\pi(1-\nu)^3} \times [3-2\hat{c}_{eq}(2-\nu)-\nu](1+2\log\rho)\cos\theta + \frac{b(1+\nu)}{2}(\bar{c}_{\max}\hat{c}_{eq})^3(1-\hat{c}_{eq})(3-4\hat{c}_{eq})\rho, \tag{73}$$

$$u_\theta^{(2)} = \frac{b\hat{c}_{eq}\bar{c}_{\max}(1+\nu)}{16\pi^2(1-\nu)^2\rho}(1-\hat{c}_{eq})(1-2\hat{c}_{eq})\sin(2\theta) + \frac{b(\hat{c}_{eq}\bar{c}_{\max})^2(1-\hat{c}_{eq})[3-2\hat{c}_{eq}(2-\nu)-\nu](1+\nu)}{8\pi(1-\nu)^3} \times (1-2\log\rho)sin\theta. \tag{74}$$

An important quantity associated with a dislocation is its line energy W. Making use of the solutions above, it is straightforward to calculate,

$$\frac{W}{W_0} = 1 - \frac{2\hat{c}_{eq}(1-\hat{c}_{eq})(1+\nu)}{1-\nu}\bar{c}_{\max}\hat{\eta} + \frac{3\hat{c}_{eq}^2(1-\hat{c}_{eq})[3-2\hat{c}_{eq}(2-\nu)-\nu]}{(1-\nu)^2}(\bar{c}_{\max}\hat{\eta})^2, \tag{75}$$

where $W_0 = \frac{Eb^2}{8\pi(1-\nu^2)}\log\frac{R}{R_0}$ is the line energy of an edge dislocation in a solid without any solute. Fig. 4 shows how dislocation line energy varies with $\hat{c}_{eq}$ for $\hat{\eta}\bar{c}_{\max} = 0.1$, 0.2 and $\nu = 0.3$. The presence of solute concentration below the saturation level, i.e. $\hat{c}_{eq} < 1$, decreases the self- energy of the dislocation. Note that the first order solution yields an underestimate of the line energy over a wide range of $\hat{c}_{eq}$.

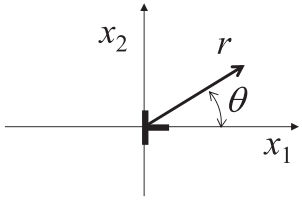

Fig. 3. A straight edge dislocation.

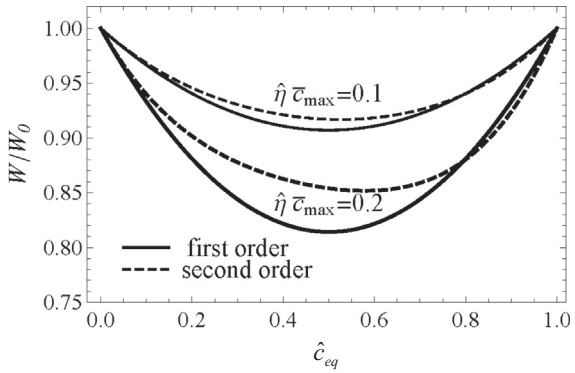

Fig. 4. Plots of dislocation line energy for $\nu = 0.3$, Eq. (75).

The solutions derived above are valid under plane strain conditions. The corresponding plane stress solutions are summarized in Appendix C.

4.3. A wedge disclination under chemical equilibrium

Consider an infinitely extended elastic medium containing a wedge disclination defined by the displacement boundary condition

$$u_\theta(r,0) - u_\theta(r,2\pi) = r\omega, \tag{76}$$

where ω is the wedge angle. Further, the solid is embedded in an infinite reservoir so that the solid is under chemical equilibrium.

Since there is no characteristic length in this problem, the formulation should remain valid for any arbitrary length scale ℓ, where $\rho = r/\ell$. Under plane strain conditions, the classical stress function

$$\hat{\varphi}_0 = -\frac{\omega}{8\pi(1-\nu^2)}\rho^2 \log\rho, \tag{77}$$

is taken as the zero order solution of the chemo-mechanical problem. The corresponding stresses are

$$\sigma_{rr}^{(0)} = -\frac{E\omega}{8\pi(1-\nu^2)}(1+2\log\rho),$$
$$\sigma_{\theta\theta}^{(0)} = -\frac{E\omega}{8\pi(1-\nu^2)}(3+2\log\rho), \sigma_{r\theta}^{(0)} = 0. \tag{78}$$

The corresponding displacement field is

$$u_r^{(0)} = \frac{\ell\rho\omega}{8\pi(1-\nu)}[1-2(1-2\nu)\log\rho] + \ell(1+\nu)\bar{c}_{\max}\hat{c}_{eq}\rho, u_\theta^{(0)} = -\frac{\rho\ell\omega\theta}{2\pi}. \tag{79}$$

The procedure to obtain the higher order stress, concentration and displacement fields are analogous to those outlined in the preceding sections. In the following, only the results are summarized here.

$$\hat{c}_1 = -(1-\hat{c}_{eq})\left[\frac{\omega(1+\log\rho)}{2\pi(1-\nu)} + \bar{c}_{\max}\hat{c}_{eq}\right], \tag{80}$$

$$\hat{\varphi}_1 = -\frac{1+\nu}{1-\nu}\bar{c}_{\max}\hat{c}_{eq}(1-\hat{c}_{eq})\hat{\varphi}_0, \tag{81}$$

$$\left[\sigma_{rr}^{(1)}, \sigma_{r\theta}^{(1)}, \sigma_{\theta\theta}^{(1)}\right] = -\frac{1+\nu}{1-\nu}\bar{c}_{\max}\hat{c}_{eq}(1-\hat{c}_{eq})\left[\sigma_{rr}^{(0)}, \sigma_{r\theta}^{(0)}, \sigma_{\theta\theta}^{(0)}\right], \tag{82}$$

$$u_r^{(1)} = -\bar{c}_{\max}\hat{c}_{eq}(1-\hat{c}_{eq})(1+\nu)\ell\rho\left[\frac{\omega(1+2\log\rho)}{8\pi(1-\nu)^2} + \bar{c}_{\max}\hat{c}_{eq}\right], \quad u_\theta^{(1)} = 0, \tag{83}$$

$$\hat{c}_2 = \bar{c}_{\max}\hat{c}_{eq}(1-\hat{c}_{eq})\frac{\omega[3-\nu-2\hat{c}_{eq}(2-\nu)]}{2\pi(1-\nu)^2}(1+\log\rho) + \frac{1}{2}(\bar{c}_{\max}\hat{c}_{eq})^2(1-\hat{c}_{eq})(3-4\hat{c}_{eq}) + (1-\hat{c}_{eq})(1-2\hat{c}_{eq})\frac{\omega^2(1+\log\rho)^2}{8\pi^2(1-\nu)^2}, \tag{84}$$

$$\hat{\varphi}_2 = \frac{\bar{c}_{\max}\hat{c}_{eq}(1-\hat{c}_{eq})}{(1-\nu)^2}\left[(1+\nu)\bar{c}_{\max}\hat{c}_{eq}(3-\nu-2(2-\nu)\hat{c}_{eq})\hat{\varphi}_0 - \frac{(1-2\hat{c}_{eq})\omega^2}{32\pi^2(1-\nu)}\rho^2(\log\rho)^2\right] \tag{85}$$

$$\sigma_{rr}^{(2)} = \frac{\bar{c}_{\max}\hat{c}_{eq}(1-\hat{c}_{eq})}{(1-\nu)^3}\left[(1-\nu^2)\bar{c}_{\max}\hat{c}_{eq}[3-\nu-2(2-\nu)\hat{c}_{eq}]\sigma_{rr}^{(0)} - \frac{(1-2\hat{c}_{eq})E\omega^2}{16\pi^2}\log\rho(1+\log\rho)\right], \tag{86}$$

$$\sigma_{\theta\theta}^{(2)} = \frac{\bar{c}_{\max}\hat{c}_{eq}(1-\hat{c}_{eq})}{(1-\nu)^3}[(1-\nu^2)\bar{c}_{\max}\hat{c}_{eq}[3-\nu-2(2-\nu)\hat{c}_{eq}]\sigma_{\theta\theta}^{(0)} - \frac{(1-2\hat{c}_{eq})E\omega^2}{16\pi^2}[1+\log\rho(3+\log\rho)], \tag{87}$$

$$\sigma_{r\theta}^{(2)} = 0, \tag{88}$$

$$u_r^{(2)} = (\bar{c}_{\max}\hat{c}_{eq})^2(1-\hat{c}_{eq})\frac{3-\nu-2\hat{c}_{eq}(2-\nu)}{8\pi(1-\nu)^3}\ell\rho\omega(1+\nu)(1+2\log\rho) + \bar{c}_{\max}\hat{c}_{eq}(1-\hat{c}_{eq})(1-2\hat{c}_{eq})\frac{\ell\rho\omega^2(1+\nu)}{16\pi^2(1-\nu)^3}[1-\nu+(1+\log\rho)\log\rho] + \frac{1}{2}(\bar{c}_{\max}\hat{c}_{eq})^3(1-\hat{c}_{eq})(3-4\hat{c}_{eq})(1+\nu)\ell\rho, \tag{89}$$

$$u_\theta^{(2)} = 0. \tag{90}$$

It seen that the stress is logarithmic singular at the disclination core $\rho = 0$. This is a much weaker singularity than the stress field at the dislocation core. In fact, the disclination line energy is bounded over any finite region encircling the core. Therefore, the line energy can be calculated as

$$W = \frac{1}{2}\int_0^R\int_0^{2\pi}(\sigma_{\rho\rho}\varepsilon_{rr}^e + \sigma_{\theta\theta}\varepsilon_{\theta\theta}^e + 2\sigma_{r\theta}\varepsilon_{r\theta}^e)d\theta dr, \tag{91}$$

where, in theory, $R \to \infty$. In practice, however, infinite crystals do not exist and R is usually taken as the size of the crystal or the distance between the disclination and other defects. If the R is taken as the characteristic length, i.e., $\ell = R$. Then, the line energy (91) can be evaluated by using the solutions derived above,

$$\frac{W}{W_0} = 1 - \frac{2\hat{c}_{eq}(1-\hat{c}_{eq})(1+\nu)}{1-\nu}\left\{\bar{c}_{\max}\hat{\eta} - \frac{\hat{c}_{eq}[7-\nu-3(3-\nu)]}{1-\nu}(\bar{c}_{\max}\hat{\eta})^2\right\}, \tag{92}$$

where

$$W_0 = \frac{E\omega^2(3-4\nu)}{64\pi(1-\nu)^2(1+\nu)},$$

is the line energy of a wedge disclination in a solid without any solute. Fig. 6 shows how the disclination line energy varies with $\hat{c}_{eq}$ for $\hat{\eta}\bar{c}_{\max} = 0.1$, 0.2 and $\nu = 0.3$. The presence of solute concentration below the saturation level, i.e. $\hat{c}_{eq} < 1$, decreases the self- energy of the dislocation. Note that, unlike in the case of dislocation, the first order solution yields an underestimate of the line energy over a wide range of $\hat{c}_{eq}$ (Figs. 3 and 5).

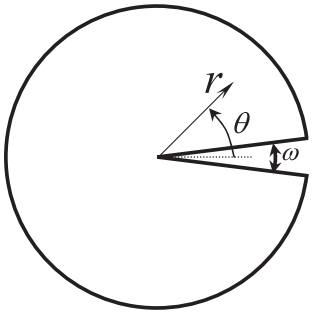

Fig. 5. A wedge disclination in an infinitely extended domain.

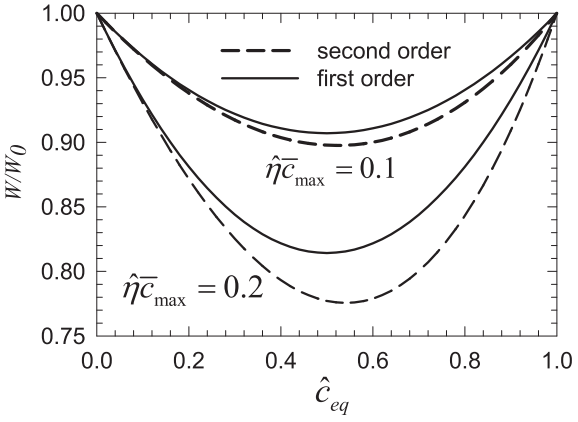

Fig. 6. Plots of disclination line energy for $\nu = 0.3$, Eq. (92).

5. Summary and conclusions

In this paper, governing equations for two-dimensional chemo-elasticity problems were formulated in terms of an Airy stress function and the solute concentration. A perturbation approach was developed to solve these equations asymptotically. This newly developed approach provides a powerful tool to solve two-dimensional chemo-elasticity problems. To illustrate the solution procedure, three fundamental problems in chemo-elasticity were solved, namely, a circular hole in an infinite plate under uniaxial tension, a straight edge dislocation and a disclination.

In addition to developing the solution methodology for two-dimensional chemo-elasticity problem, other major findings of the present study include the followings.

1. For traction-prescribed chemo-elasticity problems, the OSEC solution of Larche and Cahn (1973) corresponds to the leading term in our asymptotic solution. When the problem contains displacement boundary conditions, the OSEC solution may not yield the correct displacement fields.
2. When a plate containing a circular hole is subjected to uniaxial tension, the stress concentration near the hole is reduced unless the far-field solute concentration is greater than 50% of the solvability. In addition, the uniaxial tension leads to higher solute concentration near the equator, and lower concentration near the poles.
3. In the presence of solute concentration, the self-energy (line tension) of a straight edge dislocation could be reduced by almost 20%. This implies that dislocations in such coupled chemo-mechanical field are easier to bow out. Consequently, yield strength might be reduced.

Acknowledgments

The work is supported in part by NSF through Grant CMMI-1200075, and DoE Nuclear Energy University Program through contracts 00126931 and 00127346.

Appendix A. Open-system elastic constants

Larche and Cahn (1973, 1985) had proposed an approach that uses the open-system elastic constants (OSEC) to solve chemo-elasticity problems. In this Appendix, we will show that the OSEC approach is in essence the first order solution presented in this paper. For simplicity, we will consider only plane stress deformation. The proof for plane strain deformation can be obtained analogously.

According to Larche and Cahn (1985), the OSEC for isotropic solids are defined as

$$E^*(\hat{c}) = \frac{E}{1+\hat{\eta}\bar{c}_{\max}\hat{c}(1-\hat{c})}, \quad \nu^*(\hat{c}) = \frac{\nu - \hat{\eta}\bar{c}_{\max}\hat{c}(1-\hat{c})}{1+\hat{\eta}\bar{c}_{\max}\hat{c}(1-\hat{c})}. \tag{A.1}$$

They argue that the OSEC are "not sensitive to the composition. It is then appropriate to use the values of the open-system constants, at a composition near the average composition of the specimen". According to the notation in this paper, the "average composition of the specimen" is $\hat{c}_{eq}$. Thus, replacing $\hat{c}$ in (A.1) by $\hat{c}_{eq}$ leads to

$$E^*(\hat{c}_{eq}) = \frac{E}{1+\hat{\eta}\bar{c}_{\max}\hat{c}_{eq}(1-\hat{c}_{eq})},$$
$$\nu^*(\hat{c}_{eq}) = \frac{\nu - \hat{\eta}\bar{c}_{\max}\hat{c}_{eq}(1-\hat{c}_{eq})}{1+\hat{\eta}\bar{c}_{\max}\hat{c}_{eq}(1-\hat{c}_{eq})}. \tag{A.2}$$

Making use of (A.2) in the Hooke's law (14) and the first of (15) leads to

$$\begin{bmatrix} e_{11} \\ e_{22} \end{bmatrix} \equiv \begin{bmatrix} \varepsilon_{11} \\ \varepsilon_{22} \end{bmatrix} - \bar{c}_{\max}\hat{c}_{eq}\begin{bmatrix} 1 \\ 1 \end{bmatrix} = \frac{1}{E^*(\hat{c}_{eq})}\begin{bmatrix} 1 & -\nu^*(\hat{c}_{eq}) \\ -\nu^*(\hat{c}_{eq}) & 1 \end{bmatrix}\begin{bmatrix} \sigma_{11} \\ \sigma_{22} \end{bmatrix}, \tag{A.3}$$

$$e_{12} = \varepsilon_{12} = \frac{[1+\nu^*(\hat{c}_{eq})]\sigma_{12}}{E^*(\hat{c}_{eq})}, \tag{A.4}$$

where $e_{\alpha\beta}$ is defined as the strain with respect to the uniform deformation $\bar{c}_{\max}\hat{c}_{eq}$ induced by the uniform concentration $\hat{c}_{eq}$. If one treats $\sigma_{\alpha\beta}$ and $e_{\alpha\beta}$ as the stress and strain fields in a surrogate material with effective elastic constants $E^*(\hat{c}_{eq})$ and $\nu^*(\hat{c}_{eq})$, then the original chemo-elasticity problem can be reduced to a corresponding elasticity problem in this surrogate problem. Thus, one may simply use the existing elasticity solutions as the solutions for the corresponding chemo-elasticity problem by replacing the elastic constants with the OSEC $E^*(\hat{c}_{eq})$ and $\nu^*(\hat{c}_{eq})$. This greatly facilitates the solution to the chemo-elasticity problems.

As pointed out by Larche and Cahn (1985), the solution from the above OSEC approach is valid "far away from spinodals and critical points" since only the average solute concentration is used. Another point worth mentioning is that the strain $e_{\alpha\beta}$ obtained from the OSEC approach differs from the strain in the actual chemo-elasticity problem by $\bar{c}_{\max}\hat{c}_{eq}\delta_{\alpha\beta}$. In other words, the actual strain in the chemo-elasticity problem is $\varepsilon_{\alpha\beta} = e_{\alpha\beta} + \bar{c}_{\max}\hat{c}_{eq}\delta_{\alpha\beta}$. Thus, to obtain the displacement field for the chemo-elasticity problem, one must use $\varepsilon_{\alpha\beta}$ instead of $e_{\alpha\beta}$. This leads to difficulties in using the OSEC approach to solve chemo-elasticity problems when displacement boundary conditions are prescribed, particularly if $\hat{c}_{eq}$ is not spatially uniform.

Next, we show that the solution obtained from the OSEC approach is the first order term in the asymptotic solution obtained in this paper. To this end, we make use of (26) in (14) in conjunction with (17) to obtain

$$\begin{bmatrix}\varepsilon_{11}^{(0)}+\hat{\eta}\varepsilon_{11}^{(1)}\\ \varepsilon_{22}^{(0)}+\hat{\eta}\varepsilon_{22}^{(1)}\end{bmatrix}=\frac{1}{E}\begin{bmatrix}1 & -\nu\\ -\nu & 1\end{bmatrix}\begin{bmatrix}\sigma_{11}^{(0)}+\hat{\eta}\sigma_{11}^{(1)}\\ \sigma_{22}^{(0)}+\hat{\eta}\sigma_{22}^{(1)}\end{bmatrix}+\bar{c}_{\max}\hat{c}_{eq}(1+\hat{c}_1\hat{\eta})\begin{bmatrix}1\\1\end{bmatrix}, \tag{A.5}$$

where

$$\sigma_{11}^{(n)}=E\frac{\partial^2\hat{\varphi}_n}{\partial\bar{x}_2^2},\quad \sigma_{22}^{(n)}=E\frac{\partial^2\hat{\varphi}_n}{\partial\bar{x}_1^2},\quad n=0,1.. \tag{A.6}$$

It then follows from the second of (32) that

$$\hat{c}_1=(1-\hat{c}_{eq})\bar{\nabla}^2\hat{\varphi}_0=\frac{1-\hat{c}_{eq}}{E}\left(\sigma_{11}^{(0)}+\sigma_{22}^{(0)}\right). \tag{A.7}$$

Substituting (A.7) into (A.5) and neglecting terms containing $\hat{\eta}^2$ yield

$$\begin{bmatrix}\varepsilon_{11}^{(0)}+\hat{\eta}\varepsilon_{11}^{(1)}\\ \varepsilon_{11}^{(0)}+\hat{\eta}\varepsilon_{11}^{(1)}\end{bmatrix}-\bar{c}_{\max}\hat{c}_{eq}\begin{bmatrix}1\\1\end{bmatrix}=\frac{1}{E^*(\hat{c}_{eq})}\begin{bmatrix}1 & -\nu^*(\hat{c}_{eq})\\ -\nu^*(\hat{c}_{eq}) & 1\end{bmatrix}\begin{bmatrix}\sigma_{11}^{(0)}+\hat{\eta}\sigma_{11}^{(1)}\\ \sigma_{22}^{(0)}+\hat{\eta}\sigma_{22}^{(1)}\end{bmatrix}. \tag{A.8}$$

Comparing (A.8) with (A.3) shows that the strain and stress fields obtained from the OSEC approach are indeed the first order solutions from the asymptotic approach developed in this paper, i.e.,

$$e_{\alpha\beta}=\varepsilon_{\alpha\beta}^{(0)}+\hat{\eta}\varepsilon_{\alpha\beta}^{(1)},\quad \sigma_{\alpha\beta}=\sigma_{\alpha\beta}^{(0)}+\hat{\eta}\sigma_{\alpha\beta}^{(1)}. \tag{A.9}$$

Appendix B. Displacements in polar coordinate systems

In a polar coordinate system (ρ,θ), the displacements are related to the strains through

$$\frac{\partial\hat{u}_r}{\partial\rho}=\varepsilon_{rr},\quad \frac{\partial\hat{u}_\theta}{\partial\theta}=\rho\varepsilon_{\theta\theta}-\hat{u}_r,\quad \varepsilon_{r\theta}=\frac{1}{2}\left(\frac{1}{\rho}\frac{\partial\hat{u}_r}{\partial\theta}+\frac{\partial\hat{u}_\theta}{\partial\rho}-\frac{\hat{u}_\theta}{\rho}\right), \tag{B.1}$$

where $\hat{u}_r=u_r/\ell$, and $\hat{u}_\theta=u_\theta/\ell$. Integration of the first of (B.1) with respect to ρ in conjunction with the Hooke's law (14) gives

$$\hat{u}_r=\int\left[(1-s\nu^2)\left(\frac{\sigma_{rr}}{E}-\frac{\sigma_{\theta\theta}}{E}\frac{\nu}{1-s\nu}\right)+(1+s\nu)\bar{c}_{\max}\hat{c}\right]d\rho+f(\theta), \tag{B.2}$$

where $f(\theta)$ is an arbitrary function of θ and

$$\frac{\sigma_{rr}}{E}=\frac{1}{\rho}\frac{\partial\hat{\varphi}}{\partial\rho}+\frac{1}{\rho^2}\frac{\partial^2\hat{\varphi}}{\partial\theta^2},\quad \frac{\sigma_{\theta\theta}}{E}=\frac{\partial^2\hat{\varphi}}{\partial\rho^2},\quad \frac{\sigma_{r\theta}}{E}=-\frac{\partial}{\partial\rho}\left(\frac{1}{\rho}\frac{\partial\hat{\varphi}}{\partial\theta}\right). \tag{B.3}$$

Integration of the second of (B.1) in conjunction with (B.2) and the Hooke's law (14) gives

$$\begin{aligned}\hat{u}_\theta=&\rho\int[(1-s\nu^2)\left(-\frac{\nu}{1-s\nu}\frac{\sigma_{rr}}{E}+\frac{\sigma_{\theta\theta}}{E}\right)+(1+s\nu)\bar{c}_{\max}\hat{c}]d\theta+g(\rho)\\&-\int\int[(1-s\nu^2)\left(\frac{\sigma_{rr}}{E}-\frac{\sigma_{\theta\theta}}{E}\frac{\nu}{1-s\nu}\right)+(1+s\nu)\bar{c}_{\max}\hat{c}]d\rho d\theta+F(\theta),\end{aligned} \tag{B.4}$$

where $F(\theta)=\int f(\theta)d\theta$ and $g(\rho)$ is an arbitrary function of ρ. To determine $F(\theta)$ and $g(\rho)$, we substitute (B.2) and (B.4) into the third of (B.1) so the shear strain $\varepsilon_{r\theta}$ is expressed in terms of the displacements. We can then rewrite the first of (15) as

$$\frac{1}{2}\left(\frac{1}{\rho}\frac{\partial\hat{u}_r}{\partial\theta}+\frac{\partial\hat{u}_\theta}{\partial\rho}-\frac{\hat{u}_\theta}{\rho}\right)=\frac{\sigma_{r\theta}(1+\nu)}{E}. \tag{B.5}$$

Clearly, Eq. (B.5) depends on $\hat{\varphi}$. For the dislocation problem considered in Section 4.2, Eq. (B.5) for the zeroth order solution is

$$\sin\theta+\pi[F(\theta)-g(\rho)+\rho g'(\rho)+F''(\theta)]=0. \tag{B.6}$$

In this case, the solutions are

$$F(\theta)=\frac{\theta\cos\theta-\sin\theta}{2\pi}+C_1\cos\theta+C_2\sin\theta,\quad g(\rho)=C_3\rho. \tag{B.7}$$

For all the other cases considered in this paper, Eq. (B.5) reduces to

$$F(\theta)-g(\rho)+\rho g'(\rho)+F''(\theta)=0. \tag{B.8}$$

And, the solutions are

$$F(\theta)=C_1\cos\theta+C_2\sin\theta, g(\rho)=C_3\rho. \tag{B.9}$$

In the above, C_n, n = 1, 2, 3, are constants to be determined by the boundary conditions.

Appendix C. Dislocation solutions under plane stress conditions

$$\hat{\varphi}_0=-\frac{1}{4\pi}\rho\cos\theta\log\rho, \tag{C.1}$$

$$\sigma_{rr}^{(0)}=\sigma_{\theta\theta}^{(0)}=-\frac{E}{4\pi\rho}\cos\theta,\quad \sigma_{r\theta}^{(0)}=-\frac{E}{4\pi\rho}\sin\theta, \tag{C.2}$$

$$\begin{aligned}u_r^{(0)}=&\frac{b\cos\theta(1+\nu)}{8\pi}-\frac{b\theta\sin\theta}{2\pi}-\frac{b(1-\nu)\cos\theta\log\rho}{4\pi}\\&+\hat{c}_{eq}\bar{c}_{\max}b\rho,\end{aligned} \tag{C.3}$$

$$u_\theta^{(0)}=\frac{b(1+\nu)}{8\pi}\sin\theta-\frac{b}{2\pi}\theta\cos\theta+\frac{b(1-\nu)}{4\pi}\sin\theta\log\rho, \tag{C.4}$$

$$\hat{c}_1=(1-\hat{c}_{eq})[(1+s\nu)\bar{\nabla}^2\hat{\varphi}_0-s\bar{c}_{\max}\hat{c}_{eq}]=-(1-\hat{c}_{eq})\frac{\cos\theta}{2\pi\rho}, \tag{C.5}$$

$$\hat{\varphi}_1=-\bar{c}_{\max}\hat{c}_{eq}(1-\hat{c}_{eq})\hat{\varphi}_0, \tag{C.6}$$

$$\left[\sigma_{rr}^{(1)},\sigma_{r\theta}^{(1)},\sigma_{\theta\theta}^{(1)}\right]=-\bar{c}_{\max}\hat{c}_{eq}(1-\hat{c}_{eq})\left[\sigma_{rr}^{(0)},\sigma_{r\theta}^{(0)},\sigma_{\theta\theta}^{(0)}\right], \tag{C.7}$$

$$u_r^{(1)}=-\frac{b(1+\nu)}{8\pi}\bar{c}_{\max}\hat{c}_{eq}(1-\hat{c}_{eq})(1+2\log\rho)\cos\theta, \tag{C.8}$$

$$u_\theta^{(1)}=-\frac{b(1+\nu)}{8\pi}\bar{c}_{\max}\hat{c}_{eq}(1-\hat{c}_{eq})(1-2\log\rho)\sin\theta, \tag{C.9}$$

$$\hat{c}_2=\bar{c}_{\max}\hat{c}_{eq}\frac{(1-\hat{c}_{eq})^2}{2\pi}\frac{\cos\theta}{\rho}+\frac{(1-2\hat{c}_{eq})(1-\hat{c}_{eq})}{8\pi^2}\left(\frac{\cos\theta}{\rho}\right)^2, \tag{C.10}$$

$$\hat{\varphi}_2=(\bar{c}_{\max}\hat{c}_{eq})^2(1-\hat{c}_{eq})^2\hat{\varphi}_0-\bar{c}_{\max}\hat{c}_{eq}\frac{(1-\hat{c}_{eq})(1-2\hat{c}_{eq})}{32\pi^2}(\log\rho)^2, \tag{C.11}$$

$$\sigma_{rr}^{(2)}=\bar{c}_{\max}\hat{c}_{eq}(1-\hat{c}_{eq})\left[\bar{c}_{\max}\hat{c}_{eq}(1-\hat{c}_{eq})\sigma_{rr}^{(0)}-(1-2\hat{c}_{eq})\frac{E}{16\pi^2\rho^2}\log\rho\right], \tag{C.12}$$

$$\sigma_{\theta\theta}^{(2)}=\bar{c}_{\max}\hat{c}_{eq}(1-\hat{c}_{eq})\left[\bar{c}_{\max}\hat{c}_{eq}(1-\hat{c}_{eq})\sigma_{\theta\theta}^{(0)}-(1-2\hat{c}_{eq})\frac{E}{16\pi^2\rho^2}(1-\log\rho)\right], \tag{C.13}$$

$$\begin{aligned}&\sigma_{r\theta}^{(2)}=0,\\&u_r^{(2)}=-\hat{c}_{eq}\bar{c}_{\max}(1-\hat{c}_{eq})u_r^{(1)}-\frac{b\hat{c}_{eq}\bar{c}_{\max}}{16\pi^2\rho}(1-\hat{c}_{eq})(1-2\hat{c}_{eq})[\cos(2\theta)\\&\qquad-(1+\nu)\log\rho],\end{aligned} \tag{C.14}$$

$$u_\theta^{(2)}=-\hat{c}_{eq}\bar{c}_{\max}(1-\hat{c}_{eq})u_\theta^{(1)}+\frac{b\hat{c}_{eq}\bar{c}_{\max}}{16\pi^2\rho}(1-\hat{c}_{eq})(1-2\hat{c}_{eq})\sin(2\theta). \tag{C.15}$$

Appendix D. Disclination solutions under plane stress conditions

$$\hat{\varphi}_0 = -\frac{\omega}{8\pi}\rho^2 \log\rho, \tag{D.1}$$

$$\sigma_{rr}^{(0)} = -\frac{E\omega}{8\pi}(1+2\log\rho), \quad \sigma_{\theta\theta}^{(0)} = -\frac{E\omega}{8\pi}(3+2\log\rho), \sigma_{r\theta}^{(0)} = 0, \tag{D.2}$$

$$u_r^{(0)} = \frac{\rho\ell\omega}{8\pi}[1+\nu-2(1-\nu)\log\rho], \quad u_\theta^{(0)} = -\frac{\rho\ell\omega\theta}{2\pi}. \tag{D.3}$$

$$\hat{c}_1 = -(1-\hat{c}_{eq})\frac{\omega}{2\pi}(1+\log\rho), \hat{\varphi}_1 = -\bar{c}_{\max}\hat{c}_{eq}(1-\hat{c}_{eq})\hat{\varphi}_0, \tag{D.4}$$

$$\left[\sigma_{rr}^{(1)}, \sigma_{r\theta}^{(1)}, \sigma_{\theta\theta}^{(1)}\right] = -\bar{c}_{\max}\hat{c}_{eq}(1-\hat{c}_{eq})\left[\sigma_{rr}^{(0)}, \sigma_{r\theta}^{(0)}, \sigma_{\theta\theta}^{(0)}\right], \tag{D.5}$$

$$u_r^{(1)} = -\bar{c}_{\max}\hat{c}_{eq}(1-\hat{c}_{eq})\frac{\rho\ell\omega(1+\nu)}{8\pi}(1+2\log\rho), u_\theta^{(1)} = 0, \tag{D.6}$$

$$\hat{c}_2 = \bar{c}_{\max}\hat{c}_{eq}(1-\hat{c}_{eq})^2\frac{\omega}{2\pi}(1+\log\rho) + (1-\hat{c}_{eq})(1-2\hat{c}_{eq}) \times \frac{\omega^2}{8\pi^2}(1+\log\rho)^2, \tag{D.7}$$

$$\hat{\varphi}_2 = (\bar{c}_{\max}\hat{c}_{eq})^2(1-\hat{c}_{eq})^2\hat{\varphi}_0 - \bar{c}_{\max}\hat{c}_{eq}(1-\hat{c}_{eq})(1-2\hat{c}_{eq}) \times \frac{\omega^2}{32\pi^2}\rho^2(\log\rho)^2, \tag{D.8}$$

$$\sigma_{rr}^{(2)} = \bar{c}_{\max}\hat{c}_{eq}(1-\hat{c}_{eq})[\bar{c}_{\max}\hat{c}_{eq}(1-\hat{c}_{eq})\sigma_{rr}^{(0)} - (1-2\hat{c}_{eq})\frac{\omega^2}{16\pi^2}\log\rho(1+\log\rho)], \tag{D.9}$$

$$\sigma_{\theta\theta}^{(2)} = \bar{c}_{\max}\hat{c}_{eq}(1-\hat{c}_{eq})[\bar{c}_{\max}\hat{c}_{eq}(1-\hat{c}_{eq})\sigma_{\theta\theta}^{(0)} - (1-2\hat{c}_{eq})\frac{\omega^2}{16\pi^2}\{1+\log\rho(3+\log\rho)\}], \tag{D.10}$$

$$\sigma_{r\theta}^{(2)} = 0, \tag{D.11}$$

$$u_r^{(2)} = (\bar{c}_{\max}\hat{c}_{eq})^2(1-\hat{c}_{eq})^2\frac{\rho\ell\omega(1+\nu)}{8\pi}(1+2\log\rho) + \bar{c}_{\max}\hat{c}_{eq}(1-\hat{c}_{eq})(1-2\hat{c}_{eq})\frac{\rho\ell\omega^2}{16\pi^2}[1+(1+\nu)\log\rho(1+\log\rho)], \tag{D.12}$$

$$u_\theta^{(2)} = 0. \tag{D.13}$$

References

Bai, P., Cogswell, D.A., Bazant, M.Z., 2011. Suppression of phase separation in liFePO4 nanoparticles during battery discharge. Nano Lett. 11 (11), 4890–4896.

Burch, D., Bazant, M.Z., 2009. Size-dependent spinodal and miscibility gaps for intercalation in nanoparticles. Nano Lett. 9 (11), 3795–3800.

Cogswell, D.A., Bazant, M.Z., 2012. Coherency strain and the kinetics of phase separation in LiFePO4 nanoparticles. ACS Nano 6 (3), 2215–2225.

Cui, Z.W., Gao, F., Cui, Z.H., Qu, J.M., 2012a. A second nearest-neighbor embedded atom method interatomic potential for Li–Si alloys. J. Power Sources 207, 150–159.

Cui, Z.W., Gao, F., Qu, J.M., 2012b. A finite deformation stress-dependent chemical potential and its applications to lithium ion batteries. J. Mech. Phys. Solids 60 (7), 1280–1295.

Cui, Z.W., Gao, F., Qu, J.M., 2012c. On the perturbation solution of interface-reaction controlled diffusion in solids. Acta. Mech. Sin. 28 (4), 1049–1057.

Cui, Z.W., Gao, F., Qu, J.M., 2013a. Interface-reaction controlled diffusion in binary solids with applications to lithiation of silicon in lithium-ion batteries. J. Mech. Phys. Solids 61 (2), 293–310.

Cui, Z.W., Gao, F., Qu, J.M., 2013b. Two-phase versus two-stage versus multi-phase lithiation kinetics in silicon. Appl. Phys. Lett. 103 (14).

Fowler, R.H., Guggenheim, E.A., 1939. Statistical Thermodynamics. Cambridge University Press.

Fratzl, P., Fischer, F.D., Svoboda, J., Aizenberg, J., 2010. A kinetic model of the transformation of a micropatterned amorphous precursor into a porous single crystal. Acta Biomater. 6 (3), 1001–1005.

Graetz, J., Ahn, C.C., Yazami, R., Fultz, B., 2004. Nanocrystalline and thin film germanium electrodes with high lithium capacity and high rate capabilities. J. Electrochem. Soc. 151 (5), A698–A702.

Johnson, W.C., Huh, J.Y., 2003. Thermodynamics of stress-induced interstitial redistribution in body-centered cubic metals. Metall. Mater. Trans. A – Phys. Metall. Mater. Sci. 34A (12), 2819–2825.

Johnson, W.C., Voorhees, P.W., 1985. Equilibrium solute concentration surrounding elastically interacting precipitates. Metall. Trans. A – Phys. Metall. Mater. Sci. 16 (3), 337–347.

Kienzler, R., Fischer, F.D., Fratzl, P., 2006. On energy changes due to the formation of a circular hole in an elastic plate. Arch. Appl. Mech. 76 (11–12), 681–697.

King, K.C., Voorhees, P.W., Olson, G.B., Mura, T., 1991. Solute distribution around a coherent precipitate in a multicomponent alloy. Metall. Trans. A – Phys. Metall. Mater. Sci. 22 (10), 2199–2210.

Larche, F., Cahn, J.W., 1973. Linear theory of thermochemical equilibrium of solids under stress. Acta Metall. 21 (8), 1051–1063.

Larche, F.C., Cahn, J.W., 1985. The interactions of composition and stress in crystalline solids. Acta Metall. 33 (3), 331–357.

Sofronis, P., 1995. The influence of mobility of dissolved hydrogen on the elastic response of a metal. J. Mech. Phys. Solids 43 (9), 1385–1407.

Swaminathan, N., Qu, J., 2009. Evaluation of thermomechanical properties of non-stoichiometric gadolinium doped ceria using atomistic simulations. Modell. Simul. Mater. Sci. Eng. 17 (4), 045006.

Swaminathan, N., Qu, J., Sun, Y., 2007a. An electrochemomechanical theory of defects in ionic solids. I. Theory. Philos. Mag. 87 (11), 1705–1721.

Swaminathan, N., Qu, J., Sun, Y., 2007b. An electrochemomechanical theory of defects in ionic solids. Part II. Examples. Philos. Mag. 87 (11), 1723–1742.

Voorhees, P.W., Johnson, W.C., 2004. The thermodynamics of elastically stressed crystals. Solid State Phys.: Adv. Res. Appl. 59 (59), 1–201.